Journal of Catalysis **197,** 192–199 (2001)
doi:10.1006/jcat.2000.3067, available online at http://www.idealibrary.com on IDEAL®

Influence of Precursor Salt on Metal Particle Formation in Rh/CeO_2 Catalysts

C. Force,*[,1] J. P. Belzunegui,* J. Sanz,* A. Martínez-Arias,† and J. Soria†

*Instituto de Ciencia de Materiales de Madrid, and †Instituto de Catálisis y Petroleoquímica, CSIC, Campus Universitario de Cantoblanco, 28049 Madrid, Spain

Received July 7, 2000; revised September 14, 2000; accepted September 14, 2000

Two ceria-supported rhodium samples prepared from two different rhodium precursors (Rh (III) chloride and nitrate) are compared by CO-FTIR, EPR, and ^1H NMR with regard to their behavior toward reduction treatments under H_2. Results of IR and NMR techniques reveal that the presence of chloride ions delays rhodium reduction and favors a higher dispersion of rhodium particles at the catalyst. On the other hand, the onset of metal–support interactions (SMSI effect) upon high temperature reduction is more difficult to be established in the ex-chloride than in the ex-nitrate Rh/CeO_2 catalyst. These differences have been ascribed to the presence of Cl^- ions at the metal–support interface, which hinders electron exchanges between metal and oxide phases.

Key Words: **Rh/CeO_2 catalysts; CO-FTIR; ^1H NMR; superoxide EPR; chloride; metal–support interactions.**

INTRODUCTION

Cerium oxide has become in the past years an important promoting component in different heterogeneous catalysts, such as three-way catalysts for the elimination of pollutants from automobiles, catalysts for the removal of SO_2 from catalytic cracking flue gases or oxidation catalysts (1). The promoting effect of cerium oxide is mainly related to its ability to undergo changes in its oxidation state (within the redox couple Ce^{3+}–Ce^{4+}) with consequent formation/annihilation of surface defects (oxygen vacancies). Redox properties are substantially enhanced by formation of metal–ceria contacts, although important differences can be produced if counteranions of the precursors metal salts are partially retained during calcination procedures used during its preparation (1, 2). In particular, the presence of residual chloride decreases the extent of reduction/oxidation effects, modifying the oxygen handling properties of materials (2–9), and affecting the CO–NO conversion in rhodium-supported metal catalysts.

[1] To whom correspondence should be sent. E-mail: cforce@icmm.csic.es. Fax: 34 91 3720623.

The present work has sought to delineate the nature and extent of changes in rhodium metal particles formed upon reduction of Rh^{n+}/CeO_2 materials, prepared by wet impregnation of CeO_2 with $RhCl_3$ or $Rh(NO_3)_3$ salts. For this purpose, IR and NMR techniques, using respectively CO and H_2 as probe molecules, are employed to study changes occurring at the samples upon reducing treatments under H_2. IR spectroscopy allows differentiation between CO adsorbed on Rh ions and rhodium metal particles (10–12). On the other hand, hydrogen adsorbed on the metal is differentiated from that adsorbed on the support by NMR spectroscopy (13–15). From the analysis of the position and intensity of the shifted NMR line, the establishment of metal–support interaction was investigated (16). EPR of O_2^- formed upon oxygen adsorption on the reduced samples is employed to study changes produced at the CeO_2 surface.

EXPERIMENTAL METHODS

Two Rh/CeO_2 samples were prepared by incipient wetness impregnation of CeO_2 (Rhodia, $S_{BET} = 109\ m^2 g^{-1}$) with aqueous solutions of Rh (III) nitrate or Rh(III) chloride precursors salts (to obtain a final Rh loading of 2.5 wt%). The samples were then dried at 393 K for 24 h. These samples will be referred to as, respectively, N or Cl precursors. Following the drying step, portions of the samples were calcined under dry air flow at 673 K for 4 h (using a ramp of 4 K min^{-1}), followed by cooling down in the dry air atmosphere to 295 K. These calcined samples will be hereafter denoted as samples N and Cl, respectively.

FTIR spectra were obtained with a Nicolet 5ZDX spectrometer using a 4 cm^{-1} resolution. Thin self-supporting discs (with ca. 20 mg cm^{-2}) were prepared and introduced into a conventional pyrex cell with high-vacuum stopcocks for sample handling. In all cases, the gas phase contribution was subtracted. Reduction treatments were performed by heating under 100 Torr of H_2 at the corresponding T_r for 1 h, followed by outgassing for 30 min at the same temperature. The spectra were recorded ca. 15 min after CO exposure at

0021-9517/01 $35.00

room temperature at the indicated pressures. No significant changes were detected in any case upon increasing the exposure time. The number of scans used in each experiment was 100.

^1H NMR spectra were recorded at room temperature with a SXP 4/100 spectrometer equipped with an Aspect 2000 Fourier transform unit. The NMR frequency of proton was 67 MHz. The spectra were taken after $\pi/2$ pulse excitations (3.5 μs). The interval between successive accumulations (1 s) was chosen to avoid saturation effects. The number of accumulations (300–500) was selected to obtain a correct signal to noise ratio (S/N = 20). Intensities of the NMR lines were determined by comparing integrated intensities with that of a known external mica specimen. For NMR experiments, the samples were reduced between 373 and 773 K under dynamic conditions by using flowing H_2 (73.2 cm^3 min^{-1}). ^1H NMR spectra were taken in all cases after outgassing the H_2-reduced samples at 473 K and exposure to 10 Torr of hydrogen at room temperature.

EPR spectra were recorded at 77 K with a Bruker ER 200 D spectrometer operating in the X-band and calibrated with a DPPH standard (g = 2.0036). Portions of about 30 mg of sample were placed inside a quartz probe cell with greaseless stopcocks using a conventional high-vacuum line (capable of maintaining a dynamic vacuum of ca. 6×10^{-3} N m^{-2}) for the different treatments. The treatments under H_2 were made in static conditions by exposing the samples to 10 Torr of H_2 and heating at the corresponding temperature.

RESULTS

IR Data

FTIR spectra of the carbonyl groups, generated upon CO adsorption (50 Torr) at 298 K on samples N and Cl reduced in H_2 at different temperatures, are presented, respectively, in Figs. 1 and 2.

CO adsorption on sample N reduced at T_r = 373 K (Fig. 1a) produces two strong bands at 2061 cm^{-1} (with a small shoulder at ca. 2050 cm^{-1}) and 1996 cm^{-1} due to Rh^+ gem-dicarbonyl species (12, 17), in addition to weaker bands at 1946, 1901, and 1840 cm^{-1}, due to bridging carbonyls adsorbed on metallic rhodium particles (17–20). For the sample reduced at T_r = 573 K, a decrease in the bands at 2061 and 1996 cm^{-1}, which appear now shifted to 2070 and 2010 cm^{-1}, is observed. Besides, a shoulder at 2055 cm^{-1}, associated with linear carbonyls adsorbed on metallic rhodium (17–20), which shifts toward lower wavenumbers upon outgassing at 298 K (spectrum not shown) is now detected. Additionally, a decrease in the bands at 1946, 1901, and 1840 cm^{-1} is observed. For the sample reduced at 773 K (Fig. 1c), a strong decrease of the bands at 2070 and 2010 cm^{-1} is produced, the spectrum being

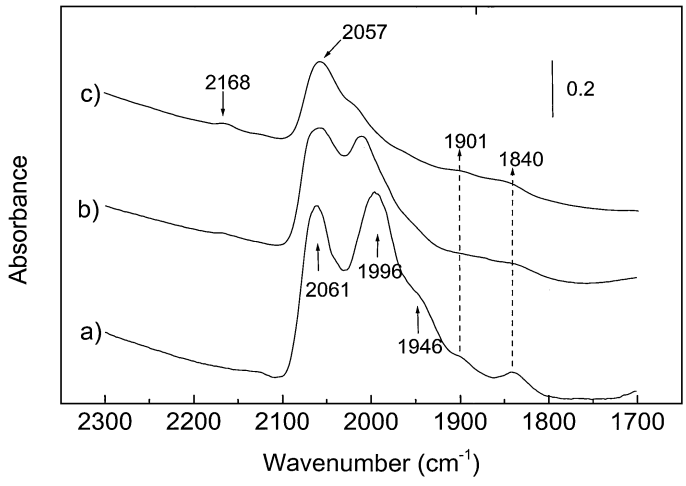

FIG. 1. FTIR spectra obtained after adsorption of CO (50 Torr) at room temperature on sample N reduced at: (a) T_r = 373 K; (b) T_r = 573 K; (c) T_r = 773 K.

formed mainly by a band at 2057 cm^{-1} with smaller shoulders at 1950, 1901, and 1840 cm^{-1}. A small band at 2168 cm^{-1} due to CO weakly adsorbed on the ceria support (21), is also observed in the spectra of the sample reduced at $T_r \geq$ 573 K.

Two strong bands at 2101 and 2035 cm^{-1}, due to Rh^+ gem-dicarbonyl species (17–20), appear after CO adsorption on sample Cl reduced at T_r = 373 K (Fig. 2a.) Noteworthy, a significantly higher overall intensity of carbonyl bands is detected in this sample with respect to sample N after the same treatment. For the sample reduced at $T_r \geq$ 573 K (Figs. 2b and 2c), new bands appear at 2071, ascribed to linear carbonyl species, and at 1950, 1910, and 1877 cm^{-1}, due to bridging carbonyls, both adsorbed on metallic rhodium particles (17–20). A strong decrease along with a certain blue shift of the bands at 2101 and 2035 cm^{-1} is produced

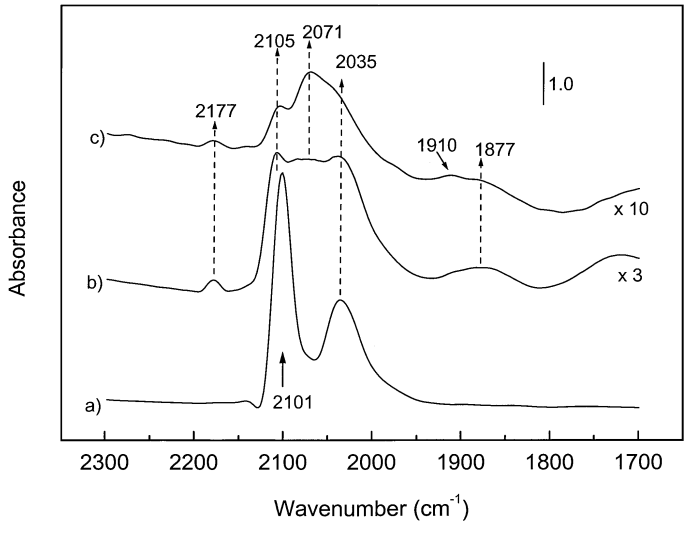

FIG. 2. As Fig. 1, for sample Cl.

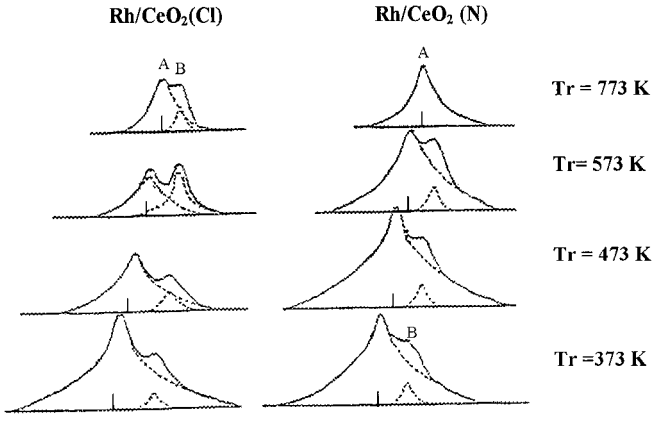

FIG. 3. ^{1}H NMR spectra of Cl and N precursors reduced at increasing temperatures (373–773 K). Following each reduction treatment, the sample was outgassed at 473 K and exposed to 10 Torr of hydrogen at room temperature.

with increasing T_r in the range 373–773 K. Additionally, a considerable decrease of bridging carbonyls is observed upon reduction at $T_r = 773$ K. A band at 2177 cm^{-1}, due to CO weakly adsorbed on the ceria support (21), also appears in this sample upon reduction at $T_r \geq 573$ K.

NMR Data

^{1}H NMR spectra following H_2 adsorption on the precursors reduced at increasing temperatures are exhibited in Fig. 3. The NMR spectra show two lines, one at the resonance frequencies (line A), associated to hydrogen adsorbed on the support, and the other shifted at higher fields (line B), associated to hydrogen adsorbed on the metal (15, 22, 23). The shift in line B is attributed to interaction of hydrogen with electrons of the metal, its position being affected by changes in metal particles size and/or by metal-support interactions (16).

Important differences, particularly for high reduction temperatures, are detected in the ^{1}H-NMR spectra of the two precursor samples. The intensity of line A (I_a) increases gradually with progress of the reduction treatment at $T_r =$ 373 K (evolution not shown) for both samples, which is attributed to hydrogen incorporation onto the support. However, reduction at $T_r =$ 473 K produces an appreciable decrease of this line for sample Cl while it slightly increases for sample N. Reduction above $T_r =$ 573 K produces a progressive decrease of line A, associated with the dehydroxylation process of the samples (24).

Figures 4 and 5 show, respectively, the intensity and chemical shift of line B produced in the course of reduction treatments. For the Cl-precursor, the intensity of line B (I_b) remains constant from $T_r =$ 373 K to 423 K and then increases greatly and exhibits a maximum at 573 K. However, for the N-precursor, it remains almost constant in the $T_r =$ 373–573 K range, at a somewhat higher value than that observed for the Cl-precursor at $T_r =$ 373 K, Figs. 3 and 4. In both cases, line B decreases when the precursors are reduced above $T_r =$ 573 K, disappearing completely at $T_r =$ 773 K for the N-precursor, Fig. 3. Additionally, a modification in the position of line B is produced during reduction treatments (Fig. 5). The shift values for the precursors reduced at $T_r =$ 373 K are, $\delta_{Cl} \cong -142$ and $\delta_N \cong -110$ ppm, remaining almost constant up to $T_r =$ 573 K; however, they decrease when the samples were reduced above 573 K, to reach values close to 60 ppm for sample Cl and tending to zero in sample N.

It was observed that the reduction characteristics of the ex-nitrate sample were essentially reproduced upon oxidation treatment at 673 K of the sample reduced at 773 K (Figs. 4 and 5). Thus, when a second reduction cycle is carried out on this oxidized sample, the intensity and chemical shift of line B observed after reduction at 373 K are similar to those measured in the first reduction cycle, except for a certain decrease of the temperature at which the line B shift starts to decrease (Fig. 5). More important differences are, however, observed in this respect for the ex-chloride sample. Thus, during the second reduction cycle (after intermediate oxidation at 673 K), intensity values are considerably higher than in the first reduction and they decrease slowly between $T_r =$ 373 and 473 K, and faster above this latter T_r. On the other hand, evolution of the shift of line B displays the same trend as that observed in the first reduction cycle although, as for the ex-nitrate sample, the temperature at which the shift starts to decrease is again lower.

EPR Data

The formation of O_2^- radicals after oxygen adsorption at 77 K, followed by EPR, has been used as a method for

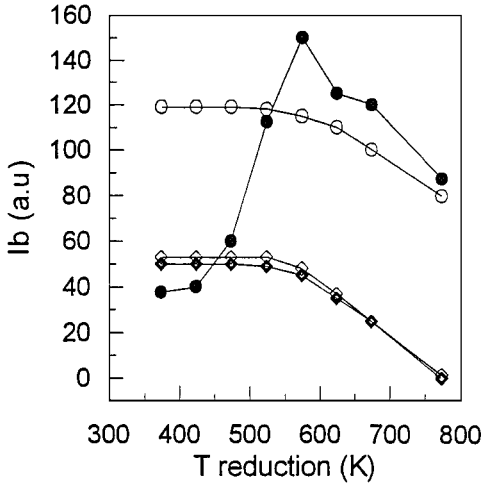

FIG. 4. Dependence of the intensity of line B (I_b) vs reduction temperature in sample Cl (●, ○) and N (◆, ◇). Full symbols correspond to reduction of the precursor samples (spectra in Fig. 3). Open symbols correspond to the reduction of the samples oxidized at 673 K after the first reduction cycle.

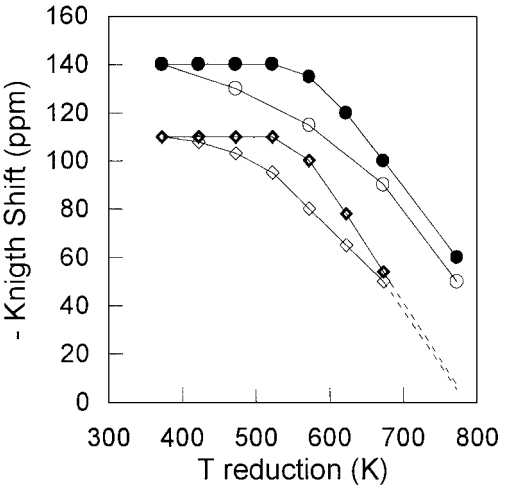

FIG. 5. Dependence of the line B shifts on reduction temperature, in samples Cl (●, ○) and N (◆, ◇). Notation for the symbols is equivalent to Fig. 4.

studying the effect of H_2 treatments on the surface of sample Cl (25).

Oxygen adsorption on sample Cl, subjected to prior calcination at 773 K and outgassing at $T_v \geq 373$ K produces a signal OC1 with $g_z = 2.026$, $g_x = 2.024$, and $g_y = 2.012$ (Fig. 6a). This signal has been also observed when chlorine is incorporated to cerium oxide in a uniform way, either by impregnation with metal chlorides or by treating CeO_2 with HCl and outgassing at 773 K (17, 26). On this basis, and considering the differences between its EPR parameters and those observed for signals of a similar kind detected on chlorine-free CeO_2 (25), as well as results of adsorption experiments employing ^{17}O-enriched oxygen mixtures (17, 26), signal OC1 is attributed to O_2^-–Ce^{4+} species affected in the Ce^{4+} coordination environment by the presence of chloride ligands (26). Signal OC1 is formed, although with variable intensity, in a wide range of prior outgassing treatments $T_v = 373$–773 K, which suggests the formation of stable species at the sample surface with chlorine coordinated to the cerium cations (26).

If, prior to O_2 adsorption, the sample calcined and outgassed at 773 K is contacted with H_2 at 298 K and outgassed at $T_v = 773$ K, the same signal OC1 is obtained. However, when the H_2 treatment is carried out at 373 K, O_2 adsorption does not produce O_2^- signals unless the sample is previously outgassed at $T_v = 473$ K. In that case, a signal OC2 is observed with $g_z = 2.028$, $g_x = 2.020$, and $g_y = 2.012$ (Fig. 6b). This signal is not stable upon subsequent warming at 298 K, a small signal OC1 being observed after that treatment. Signal OC2 had been also observed for a CeO_2 sample treated with HCl, outgassed at $T_v \leq 773$ K, and contacted with O_2 (26). This signal, as OC1, has been assigned to O_2^-–Ce^{4+} species with chloride coordinated to cerium cations; however, the number of chloride ligands coordinated to the cerium cations must be lower in this case than for signal OC1 (26). When the H_2 treatment is carried out at $T_r = 473$–573 K, O_2 adsorption produces a signal O3, with $g_z = 2.030$, $g_y = 2.016$, and $g_x = 2.012$, when the sample is previously outgassed at 298 K (Fig. 6c), signal OC2 predominating if it is previously outgassed at $T_v = 373$ K. Signal O3 is similar to that observed for O_2^-–Ce^{4+} species located at isolated oxygen vacancies formed in chlorine- free CeO_2 (25). If the H_2 treatment is carried out at $T_r = 673$–773 K, O_2 adsorption produces again signal

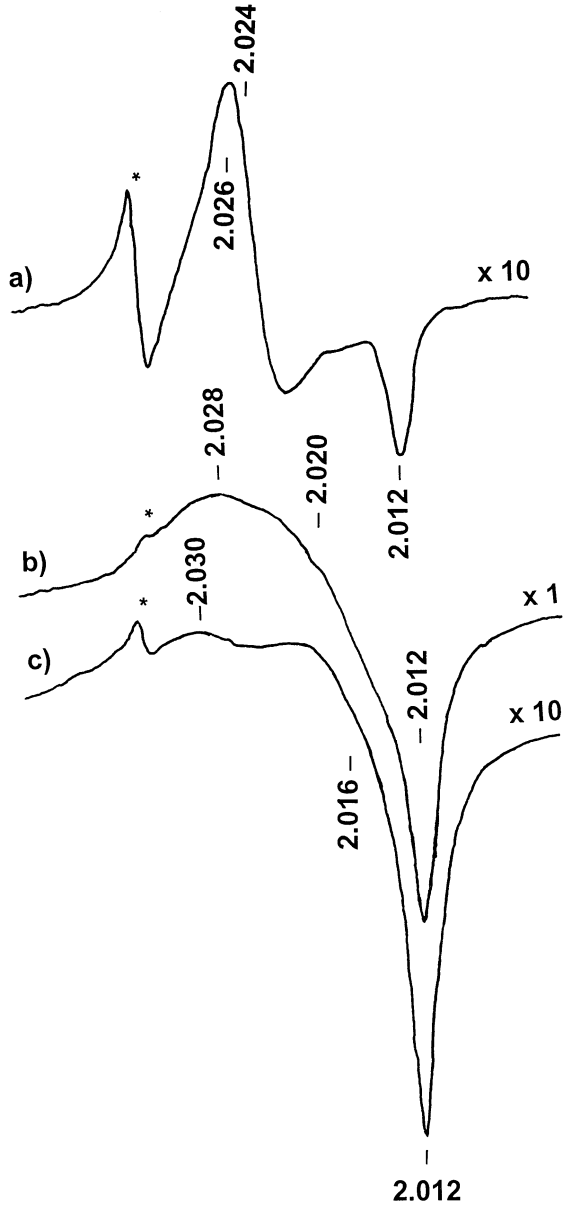

FIG. 6. EPR spectra of sample Cl calcined at 773 K after oxygen adsorption at 77 K on the sample: (a) previously outgassed at 773 K; (b) reduced at 373 K and outgassed at 473 K; and (c) previously reduced at 473 K and outgassed at 298 K. Asterisk marks correspond to a Mn^{2+} impurity signal.

O3 when the sample was preoutgassed at $T_v = 298$–373 K, while signal OC2 predominates for higher preoutgassing temperatures. For these latter cases, signal OC1 is detected with a small intensity only when the sample is warmed at 373 K.

DISCUSSION

Metal Particles Formation

Generation of Rh metal particles in Rh/CeO_2 precursors must involve reduction of Rh^{3+} ions incorporated during CeO_2 impregnation. In the case of the ex-nitrate sample, the thermal reduction process must involve concomitant evolution of nitrogen (as N_2, NO_x, or NH_3) and H_2O; however, elimination of chlorine (as Cl_2 or ClH) is more difficult in ex-chloride samples, as shown by a previous XPS study (27); indeed, that XPS study confirmed the presence of chloride ions for the Cl-precursor sample independently of its submission to reduction or O_2 calcination treatments (27).

During reduction of Rh/CeO_2 catalysts, incorporation of hydrogen into the support is favored by spillover from the rhodium metal particles (28). The incorporation of hydrogen at $T_r = 373$ K favors the formation of OH^- groups, as evidenced by NMR (Fig. 3), and the reduction of Ce^{4+} to Ce^{3+} in ceria (1, 29). This constitutes the first step in the reduction of the sample, as shown in Scheme 1. With increasing the reduction temperature, these OH^- groups are expected to be progressively eliminated with formation of anion vacancies (Scheme 1). However, analysis by NMR of the evolution of line A with reduction temperature for Rh/CeO_2 precursors showed that the elimination of OH^- is produced at lower T_r for the Cl than for the N precursor. This fact suggests that the presence of Cl^- ions can produce a destabilization of OH^- groups, probably induced by a process of exchange of OH^- by Cl^- (as shown by mechanism B in Scheme 1). This process would explain the observed decrease of line A upon reduction of the Cl precursor at $T_r \geq 473$ K, which contrasts with the behavior observed for the N precursor, where OH^- groups are stable up to 673 K. In this sense, previous work by Bernal *et al.* (29) has shown the incorporation of Cl^- ions into oxygen vacancies, particularly upon high-temperature reduction, leading to formation of "$Ce^{3+}OCl$" entities at the CeO_2 surface, in agreement with mechanism B proposed in Scheme 1. The Cl^- incorporation to the support is consistent with observation of signals OC1 and OC2 in the EPR spectra and explain the slow decrease observed Cl^- content detected in ex-chloride precursor during metal particles formation.

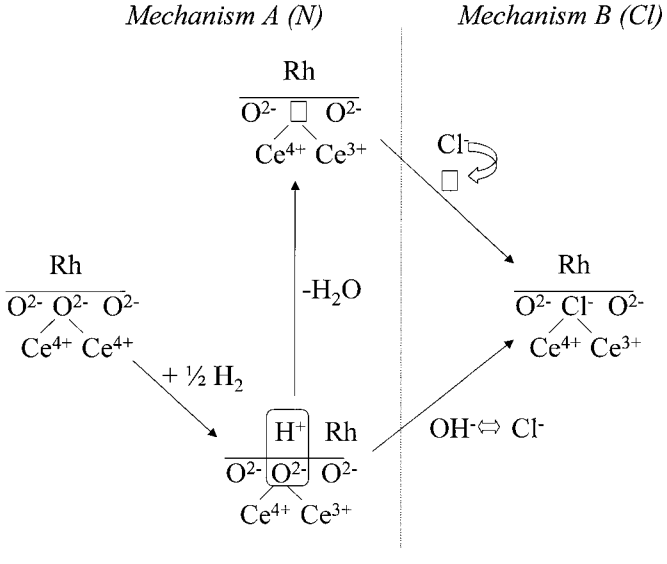

SCHEME 1

Considering that for the N-precursor (both after the initial or the second reduction cycle), the intensity of the NMR line B remains constant between $T_r = 373$ and $T_r = 573$ K and decreases above this temperature (Figs. 3 and 4), it can be assumed that most of the rhodium has been reduced, with concomitant metal particles formation, already at $T_r = 373$ K. This is consistent with observation of bridging carbonyls in the IR spectrum, Fig. 1a, although the presence of Rh^+ dicarbonyl bands suggests that a part of the rhodium could still remain in an oxidized state after that reduction treatment.

In the case of the Cl precursor, NMR results (Figs. 3 and 4) show that line B appears already for $T_r = 373$ K, which indicates that at least a part of the rhodium is easily reducible and forms metal particles at $T_r = 373$ K. However, the large increase of I_b produced upon increasing T_r from 423 to 573 K, indicates that a larger part of the Rh, in comparison to sample N, is stabilized in oxidized states, requiring $T_r > 423$ K for its reduction and formation of metal particles. The difference between the two samples can be explained by assuming that a certain amount of rhodium is stabilized in a cationic state by interaction with chlorine anions in the Cl precursor. The same effect is also suggested by comparison of samples N and Cl by FTIR (Figs. 1 and 2). The important intensity of the Rh^+ carbonyls bands and the absence of Rh^0 carbonyl bands in sample Cl reduced at $T_r = 373$ K, in contrast to sample N, can be related to a lower reduction degree of rhodium for sample Cl than for sample N at that T_r. It must be, however, considered that CO adsorption on the smaller particles present in the ex-chloride sample (as discussed below) can proceed to a certain extent by an oxidative rupture process of CO adsorbed, producing rhodium oxidation (30, 31), a process which might be favored by the presence of chloride (32). On the other hand, the higher frequency of the gem-dicarbonyl bands for sample Cl can be ascribed, as discussed in a previous report (17), to an effect of the higher electronegativity of chloride with respect to oxide ligands, suggesting that those anions

could act as anchoring entities between rhodium and the support (33).

Rhodium Dispersion

From the analysis of the line B shift (δ) in the ^1H NMR spectra (Fig. 5), it is possible to estimate metal dispersions, because that value is directly related to the metal particle size (34–37). In the case of small rhodium particles, large δ values are observed (−200 ppm). However, when the metal particle grows, the electron spin density at surface local sites decreases and δ decreases to −125 ppm (37). A comparison of δ values in Rh/CeO_2 catalysts reduced at $T_r = 373$ K indicates that the size of particles formed in ex-chloride Rh/CeO_2 (−140 ppm) is smaller than in ex-nitrate Rh/CeO_2 (−110 ppm). A similar conclusion is reached when analyzing I_b in the two precursors as the intensity achieved after full rhodium reduction for the Cl precursor (at $T_r \geq 473$ K) is significantly higher than that observed for the *N* precursor, indicating a higher dispersion, which can be associated with a lower particle size, in the former.

During the second reduction cycle of samples oxidized at 673 K, the evolution of I_b is qualitatively similar in both catalysts, decreasing with increasing the T_r (Fig. 4). The results obtained during subsequent reduction cycles (with intermediate oxidation at 673 K in each case) did not show significant differences with those obtained in the second cycle. These results indicate that the reduction of oxidized Rh, once metal particles have been previously created during a former reduction cycle, is not retarded by the presence of chlorine in sample Cl, probably because a Cl^- migration to support sites not directly interacting with the rhodium particles is produced during the redox cycling. This could proceed through migration of chlorine into subsurface ceria layers and its stabilization by formation of cerium oxychloride-type microphases (29). Generation during the reduction of the support of surface sites free of chloride influence, likely located near the rhodium metal particles, is in agreement with formation of signal OC3 in the EPR spectra of sample Cl reduced at $T_r \geq 473$ K. In this respect, analysis of the evolution of the characteristics of O_2^- radicals with T_r, which show the formation of signal OC1 for $T_r = 298$ K, while signals OC2 and OC3 appear for, respectively, $T_r = 373$ K and $T_r \geq 473$ K, suggests that chlorine migration toward sites apart from the rhodium particles follows a gradual process whose extent increases with T_r.

On the other hand, achievement of similar values of I_b during the second and subsequent reduction cycles for each of the samples suggests that no important sintering of the metal particles is produced upon reduction. The higher values of I_b and δ for the ex-chloride sample indicate that a higher rhodium dispersion is achieved for the ex-chloride than for the ex-nitrate sample. Metal dispersion values can be determined from I_b values, once calibrated with an external standard. Thus, following adsorption of 10 Torr of H_2 at room temperature on samples oxidized at 673 K, reduced at 473 K and outgassed at 473 K the dispersions obtained from this analysis are 0.40, and 0.78, for, respectively, samples N and Cl, which would correspond to particle sizes of ca. 25 and 13Å, respectively. On the other hand, the presence of a considerable amount of highly dispersed rhodium (probably associated with particle sizes ≤10 Å), is responsible for the important line B detected in the Cl-precursor reduced at $T_r = 573$ K (Figs. 3 and 4). The higher rhodium dispersion in sample Cl with respect to sample N is also consistent with the comparatively larger intensity of carbonyl species observed for the former after reduction at $T_r = 373$ K (Figs. 1 and 2). On the basis of the presented results, it can be concluded that the presence of Cl^- ions at the ceria surface favors Rh dispersion in CeO_2 samples.

Metal–Support Interaction

For both samples Cl and N, it is observed that the intensity of the FTIR bands corresponding to bridging carbonyls adsorbed on metal particles decreases when the samples are reduced at $T_r \geq 573$ K (Figs. 1 and 2). In parallel, the intensity of NMR line B, due to hydrogen adsorbed on the metal particles, also decreases for that T_r (Figs. 3 and 4). This decrease in the amounts of CO or H_2 adsorbed on metal particles could be explained by two different processes: (i) sintering of metal particles; and (ii) generation of strong metal–support interactions (SMSI). In the present case, achievement of reproducible I_b values after consecutive reduction/oxidation cycles (following the first reduction cycle) suggests that no important particle sintering is produced in the course of reduction, leaving metal–support interactions as the most likely explanation for the observed results.

These metal–support interactions might be due either to the existence of metal–support electronic interactions or to an effect of coverage of the metal particles by support suboxide species, or to both (16). These interactions would affect the electron density at the metal surface sites, modifying the observed line B shift, which decreases when the extent of SMSI effects increases (16, 38). The plot of the line B shift vs T_r shows that the shift decreases more markedly in sample N than in sample Cl, indicating that the electronic perturbation is more important in the first case. Taking into account that the rhodium particles are smaller in ex-chloride than in ex-nitrate samples, the metal–support interactions should, in principle, be favored in the former case (16, 38). However, the electronic perturbation detected in sample Cl is lower, indicating that other effects affect the onset of the SMSI effects. In agreement with these arguments, the incorporation of Cl^- to the support could

hinder electron exchanges between both phases, explaining the observed SMSI delay in sample Cl. It should be noted that in spite of the mentioned fact that chlorine migration from the metal–support interface regions must be produced in the course of the reduction of the Cl-precursor, SMSI effects are only partially achieved for the ex-chloride sample (independently of the reduction cycle), suggesting that the interface support regions responsible for the SMSI effects might involve several atomic layers around the rhodium particles.

Considering the marked influence that anion vacancies at the metal–support interface have on the electronic perturbation of metal particles, the observed decrease of intensity and shift of line B could be associated with an electronic perturbation produced in the metal particles by the reduced support during establishment of the SMSI effect. The generation of stable oxygen vacancies at the metal–support interface should facilitate an easier onset of SMSI effects, decreasing the temperature at which this observation is produced. In the case of sample N, these effects produce an important decrease on intensity and shift of line B after reduction at 773 K (Figs. 4 and 5). The extent of this effect is more moderate in sample Cl, showing that the chlorine removal from the metal–support interface and its incorporation in deeper CeO_2 layers, is a slow process at the temperatures used in this work. The effects taking place at the metal–support interface will also depend on the interface surface, which will increase if a cerium suboxide overlayer starts to cover the metal particles upon operation of SMSI effects, a process which can be involved to a greater extent for sample N.

CONCLUSIONS

IR, NMR, and EPR techniques have been used to analyze reduction under H_2 of Rh/CeO_2 catalysts prepared from chloride and nitrate precursor salts. The results show an easier rhodium reduction for the ex-nitrate than for the ex-chloride precursor sample, which is attributed to a chloride-induced stabilization of cationic rhodium species. This chloride influence on rhodium reduction is eliminated by subjecting the sample to high temperature reduction followed by oxidation at 673 K, which is attributed to chlorine migration to sites apart from the metal–support region produced during the reduction process. On the other hand, the results show that the presence of chloride favors rhodium dispersion in the ex-chloride Rh/CeO_2 catalyst.

The metal–support interaction (SMSI effect), produced upon high temperature reduction of the samples, is responsible for the observed decrease on H_2 and CO adsorption. The electronic perturbation of the metal by the reduced support, which is involved in this SMSI effect, is more favored in the ex-nitrate sample, which is attributed to a certain hindering on metal–support electronic effects induced by the presence of chlorine in the ex-chloride sample.

ACKNOWLEDGMENTS

Financial support from CICYT under project MAT98-0971 is acknowledged. C.F. is grateful to Volkswagen-Audi-CSIC for the grant received. A.M.-A. thanks the "Comunidad de Madrid" for a postdoctoral grant under which this work was carried out. We are grateful to Prof. G. Munuera for fretful discussions

REFERENCES

1. Trovarelli, A., *Catal. Rev. Sci. Eng.* **38**, 439 (1996).
2. Bernal, S., Calvino, J. J., Cifredo, G. A., Gatica, J. M., Pérez Omil, J. A., Laachir, A., and Perrichon, V., *Stud. Surf. Sci. Catal.* **96**, 419 (1995).
3. Cunningham, J., Cullinane, D., Sanz, J., Rojo, J. M., Soria, J., and Fierro, J. L. G., *J. Chem. Soc. Faraday Trans.* **88**, 3233 (1992).
4. Kondarides, D. I., and Verykios, X. E., *J. Catal.* **174**, 52 (1998).
5. Cunningham, J., Hickey, N., Cataluña, R., Conesa, J. C., Soria, J., and Martínez-Arias, A., *Stud. Surf. Sci. Catal.* **101**, 681 (1996).
6. Kepinski, L., Wolcyrz, M., and Okal, J., *J. Chem. Soc. Faraday Trans.* **91**, 507 (1995).
7. Cunningham, J., O'Brien, S., Sanz, J., Rojo, J. M., Soria, J., and Fierro, J. L. G., *J. Mol. Catal.* **57**, 379 (1990).
8. Salasc, S., Perrichon, V., Primet, M., Chevrier, M., Mathis, F., and Moral, M., *Catal. Today* **50**, 227 (1999).
9. Badri, A., Binet, C., and Lavalley, J. C., *J. Phys. Chem.* **100**, 8363 (1996).
10. Kondarides, D. I., Zhang, Z., and Verykios, X. E., *J. Catal.* **176**, 536 (1998).
11. Soria, J., Martínez-Arias, A., Fierro, J. L. G., and Conesa, J. C., *Vacuum* **46**, 1201 (1995).
12. Martínez-Arias, A., Soria, J., and Conesa, J. C., *J. Catal.* **168**, 364 (1997).
13. Reineke, N., and Haul, R., *J. Phys. Chem.* **88**, 1232 (1984).
14. Fraissard, J., *Catal. Today* **51**, 481 (1999).
15. Sanz, J., and Rojo, J. M., *J. Phys. Chem.* **89**, 4974 (1985).
16. Belzunegui, J. P., Sanz, J., and Rojo, J. M., *J. Am. Chem. Soc.* **112**, 4067 (1990).
17. Soria, J., Martínez-Arias, A., Coronado, J. M., and Conesa, J. C., *Topics Catal.* **11/12**, 205 (2000).
18. Rice, C. A., Worley, S. D., Curtis, C. W., Guin, J. A., and Tarrer, A. R., *J. Chem. Phys.* **74**, 6487 (1981).
19. Worley, S. D., Rice, C. A., Mattson, G. A., Curtis, W. C., Guin, J. A., and Tarrer, A. R., *J. Chem. Phys.* **76**, 20 (1982).
20. Cavanagh, R. R., and Yates, J. T., *J. Chem. Phys.* **74**, 4150 (1981).
21. Li, C., Sakata, Y., Arai, T., Domen, K., Maruya, K., and Onishi, T., *J. Chem. Soc. Faraday Trans. 1* **85**, 929 (1989).
22. Rouabah, D., Benslama, R., and Fraissard, J., *Chem. Phys. Lett.* **179**, 218 (1991).
23. Menorval, L. C., and Fraissard, J., *in* "Growth and Properties of Metal Clusters" (J. Bourdon, Ed.), p. 151. Elsevier, Amsterdam, 1980.
24. Belzunegui, J. P., Sanz, J., and Rojo, J. M., *J. Am. Chem. Soc.* **114**, 6749 (1992).
25. Soria, J., Martínez-Arias, A., and Conesa, J. C., *J. Chem. Soc. Faraday Trans.* **91**, 1669 (1995).
26. Soria, J., Conesa, J. C., and Martínez-Arias, A., *Coll. Surf. A* **158**, 67 (1999).
27. Holgado, J. P., and Munuera, G., *Stud. Surf. Sci. Catal.* **96**, 109 (1995).
28. Zafiris, G. S., and Gorte, R. J., *J. Catal.* **139**, 561 (1993).
29. Bernal, S., Botana, F. J., Calvino, J. J., Cauqui, M. A., Cifredo, G. A., Jorbacho, A., Pintado, J., and Rodriguez Izquierdo, J. M., *J. Phys. Chem.* **97**, 4118 (1993).

30. van't Blik, H. F. J., van Zon, J. B. A. D., Huizinga, T., Vis, J. C., Koningsberger, D. C., and Prins, R., *J. Am. Chem. Soc.* **107**, 3139 (1985).
31. Solymosi, F., and Pásztor, M., *J. Phys. Chem.* **89**, 4789 (1985).
32. Johnston, P., and Joyner, R. W., *J. Chem. Soc. Faraday Trans.* **89**, 893 (1993).
33. (a) Keyes, M. P., and Watters, K. L., *J. Catal.* **110**, 96 (1988); (b) Munuera, G., González-Elipe, A., Espinós, J. P., Muñoz, A., Conesa, J. C., Soria, J., and Sanz, J., *Catal. Today* **2**, 663 (1988).
34. (a) Denton, R., Muhlschlegel, B., and Scalatpio, D., *Phys. Rev. Lett.* **26**, 707 (1971); (b) Kubo, R. J., *Phys. Soc. Jpn.* **17**, 975 (1962).
35. Stokes, T. H., Makowka, D. C., Wang, P. K., Rudaz, L. S., and Slichter, C. P., *J. Mol. Catal.* **20**, 321 (1983).
36. Sanz, J., Force, C., Bernal, S., Gatica, J. M., and Guil, J. M., Langmuir, in press.
37. Chang, T.-H., Cheng, C.-P., and Chuin, T.-Y., *J. Catal.* **138**, 457 (1992).
38. Tauster, S. J., *Acc. Chem. Res.* **20**, 389 (1987).